MELLIN-FOURIER CORRELATION

By

EDWARD CARNEY FRIDAY

A DISSERTATION PRESENTED TO THE GRADUATE SCHOOL
OF THE UNIVERSITY OF FLORIDA IN
PARTIAL FULFILLMENT OF THE REQUIREMENTS
FOR THE DEGREE OF DOCTOR OF PHILOSOPHY

UNIVERSITY OF FLORIDA

1985

ACKNOWLEDGMENTS

The author wishes to thank Dr. Henry Register for his encouragement to pursue graduate studies at the University of Florida. Dr. Roland Anderson has provided counseling and essential critical review during the years of experimental effort leading to publication. The Air Force Office of Scientific Research provided initial funding for this research through the basic research program conducted by the Air Force Armament Laboratory at Eglin Air Force Base, Florida. The final stages of the research would have been impossible without the computing and word processing resources provided by E G & G Special Projects, Incorporated.

TABLE OF CONTENTS

		Page
ACKNOWLEDGMENTS		iii
ABSTRACT		v
CHAPTERS		
I	INTRODUCTION	1
	Limitations of Classical Techniques	1
	The Mellin-Fourier Correlation Process	1
	Results Obtained by Other Workers	7
	Areas Investigated in this Work	9
II	BACKGROUND	12
	Experimental Techniques	12
	Theory For Extending the Normal Scale Invariance	18
III	APPLYING OPTIMUM SAMPLING TECHNIQUES	26
	Examples of Optimum Sampling	26
	Testing Theoretical Predictions	44
IV	ADDITIONAL EXPERIMENTS	52
	Higher Space Bandwidth	52
	Adding Noise	56
V	CONCLUSIONS	65
REFERENCES		69
BIOGRAPHICAL SKETCH		70

Abstract of Dissertation Presented to the Graduate School of the University of Florida in Partial Fulfillment of the Requirements for the Degree of Doctor of Philosophy

MELLIN-FOURIER CORRELATION

By

Edward Carney Friday

May 1985

Chairman: Roland C. Anderson
Major Department: Engineering Sciences

This dissertation evaluates the success of a pattern recognition system which attempts to recognize an object even though the object differs in size and orientation from the object used as a reference. The criteria for recognition were the peak value and shape of the cross correlation function calculated in two dimensions. The cross correlation was performed using Fourier transform techniques to judge the utility of implementing the system using many standard optical components. Size, or scale, invariance was achieved using a logarithmic sampling technique (the Mellin transform), and variations on traditional sampling methods were shown to extend the scale

invariance predicted by previous reseachers. The utility of the sampling techniques developed was proven using images acquired from infrared sensors carried aboard helicopters. Limits of practical scale invariance were explored and system design approaches were suggested from the results of numerical experiments carried out in computer simulations.

CHAPTER I
INTRODUCTION

Limitations of Classical Techniques

Pattern recognition is often performed in autonomous hardware by comparing imagery from an on-board sensor with an ideal or reference image stored in a memory. Military systems frequently are required to recognize patterns even though they are slightly different from the reference for which the system was designed. Signal processing techniques to overcome certain types of distortions in sensed imagery have been described in the literature (1). The most common distortions are scale and orientation changes. Classical matched filters are unreliable unless the reference and sensed objects are very nearly the same. When the peak signal to RMS noise ratio (SNR) of the correlation function is used as a figure of merit for the holographic matched filter technique, losses in SNR of 27 db can occur with as little as 2% scale difference and 3.5 degrees of orientation difference (2).

The Mellin-Fourier Correlation Process

Distortions such as scale changes and rotations of the pattern of the sensed image may be overcome by using the proper choice of geometrical transformations. Since most

scale invariant transformations are not invariant to translation, the Fourier transform magnitude is sometimes used as the first step in a pattern matching scheme to achieve shift invariance before the scale invariant geometrical transformation is performed. The scale invariant transformation is achieved in practice by resampling the original image. This resampling process causes spatial distortion, e.g. warping, and is therefore sometimes called space variant. Figure 1 shows the process used to achieve Mellin-Fourier (scale and shift invariant) correlation between a reference image and a sensed image. The first step is to calculate the magnitude of the Fourier transform of the reference and sensed images. The Mellin transform is not invariant to object translation, so pattern recognition using Mellin transforms is usually done using the magnitude of the Fourier transform of an object. This technique uses the shift invariance of the Fourier transform to provide a centered image for later exponential resampling. The magnitude of the Fourier transform is equivalent to the diffraction pattern obtained when an image is used as the aperture of an optical system. This pattern contains no phase, i.e. position, information, and as a result is invariant to the position of the pattern within the system field of view.

The next step in the Mellin-Fourier correlation process is to perform the geometrical transformation necessary to

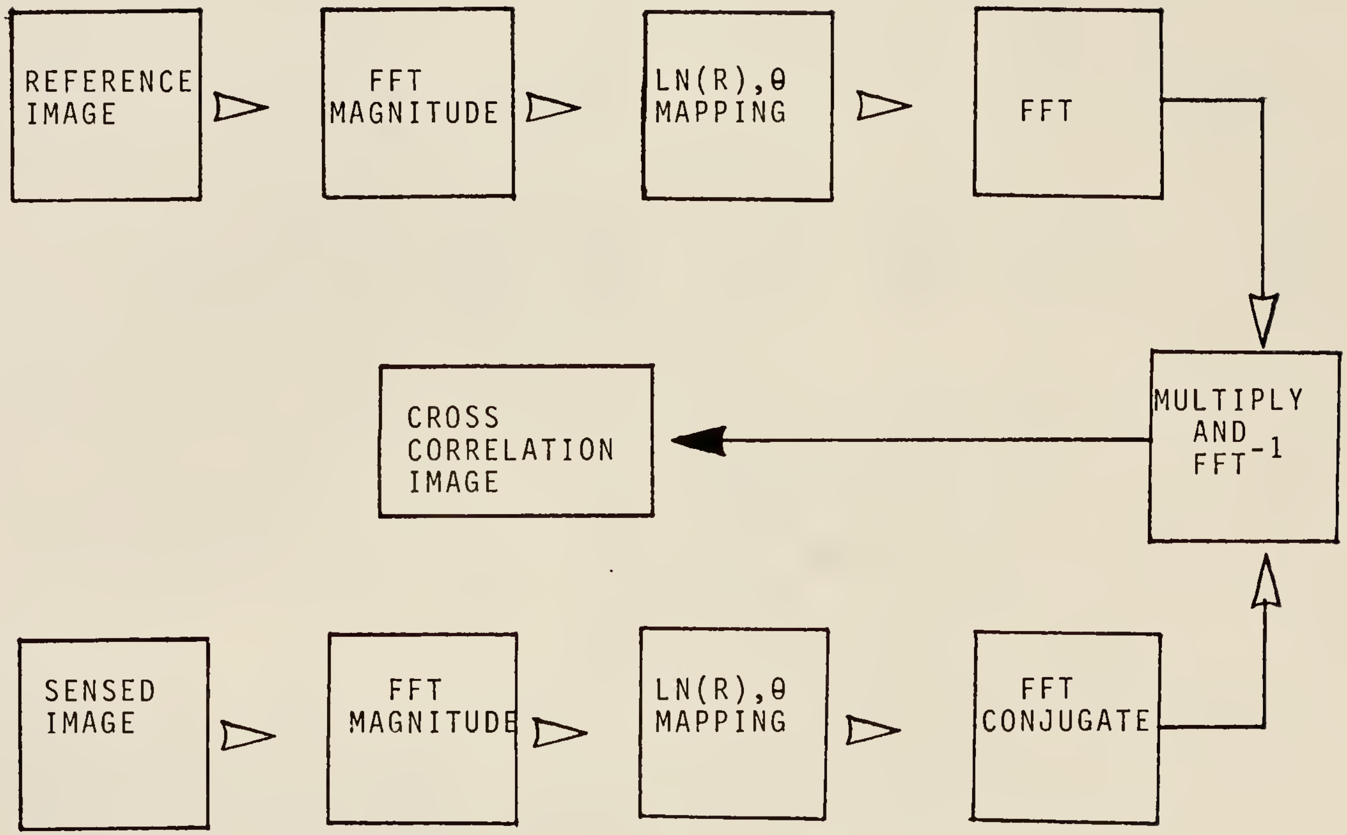

Figure 1. The Mellin-Fourier correlation process

create an image which has a useful relationship to scale changes in the input image. The geometric transformation used in this research maps the Fourier transform polar plane into a rectangular plane. The orthogonal axes in the new rectangular coordinate system are defined as the logarithm of radial distance and the polar angle in the original Fourier transform plane. These axes are denoted as ln (R) and θ, respectively. The quantity R is the radial distance from the zero frequency, or d.c. term. The natural logarithm of R is used in the transformation because a multiplicative scale change occurring in the Fourier transform plane causes a linear shift in the ln (R) axis. The quantity θ is the angle measured counterclockwise from the horizontal axis. When a Fourier transform image is mapped using this geometric transformation, a new image plane is created with each location in the ln (R),θ plane corresponding to one or more locations in the Fourier transform plane. Figure 2 shows what happens in the ln(R),θ plane when a scale change occurs in the original image. The top image in Figure 2 is the ln(R),θ image generated by a 10 x 10 reference square. The ln(R),θ images below it are sensed images with various scale changes present. As the scale of the sensed image changes, the pattern in the ln(R),θ image simply translates. Features in the ln(R),θ

Figure 2. Effect of scale changes on the ln(R),θ image

image do not change size as they would in the Fourier transform image. It is this scale-to-translation property of the ln(R),θ mapping that is exploited in the scale invariant Mellin-Fourier correlator.

The final step in Mellin-Fourier correlation is a standard cross correlation calculation performed with the ln(R),θ reference and sensed images as inputs. The correlator in this work is implemented with a computer simulation, and cross correlation is performed using transform techniques rather than by direct calculation. This technique requires fewer calculations than cross correlation performed directly. The output of the Mellin-Fourier correlator is a cross correlation image with a peak value whose X coordinate reveals the amount of scale change between the reference and sensed images. The Y coordinate of the cross correlation peak gives the amount of rotation difference between the reference and sensed images. This work is concerned with considerations in sampling the ln(R),θ image and the scale invariance expected of a system using the sequence of operations described in Figure 1. In addition, the effects of noise added to the reference and sensed images on the shape and amplitude of the cross correlation image are determined.

Results Obtained by Other Workers

Cassasent and Psaltis (3) have shown how space variant processors can be used to perform scale invariant correlation. With their technique, scale and rotation changes in a sensed pattern were converted into a translation by use of the logarithmic coordinate transformation described above. Standard shift invariant correlation methods, i.e., Fourier transform methods, were then used for pattern recognition of the scaled function.

An analysis performed by Cassasent and Psaltis showed that the spatial distortion introduced by the logarithmic transformation resulted in increased space bandwidth requirements. The logarithmic coordinate transformation is equivalent to resampling an image at exponentially spaced intervals, and the increase in space bandwidth (number of samples) is caused by the oversampling which takes place at small values of the input coordinate. Their analysis considered the increased sampling requirements imposed by a function which moved partially out of the sampled domain when scaled by a factor A. This loss of information gave rise to inaccuracies. Space bandwidth requirements were said to increase by a factor of 5.3 when 100% scale change (A=2) was accommodated (3).

Analysis done by Anderson and Callary (4) involved a function which remained entirely within the sampled domain when scaled by a factor A. In this case, there were no inaccuracies introduced because the function was defined to be zero outside the domain of interest, and no information about the function was lost when scale changes occurred. They showed that the increase in space bandwidth could be minimized by careful choice of the constants used in the logarithmic coordinate transformation. In their scheme, oversampling at small values of radial distance was governed by meeting the Nyquist criterion at the widest sampling interval, and by oversampling only to the extent necessary to accommodate the predicted scale change. Using this scheme, space bandwidth requirements increased by a factor of only 2.7 when accommodating a 100% scale change.

Variations of this geometrical transformation scheme have been reported by other researchers (5). In those studies, the location of the correlation peak in the Mellin-Fourier correlation plane was used to identify the actual scale change and rotation of the sensed image. Then,a new reference image was synthesized at the proper scale and rotation angle for application of traditional correlation schemes.

Areas Investigated in this Work

This study evaluates the success of a pattern recognition system which attempts to recognize objects in a sensed image which differ in scale and rotation from the reference image. The intent is to establish the limits of use for the Mellin-Fourier correlation techniques rather than to design a specific algorithm for pattern recognition. Experience has shown that such algorithms are very dependent upon a system application.

The approach used here was to calculate sampling requirements based on a desired range of scale invariance, and then to use a computer simulation of the correlation process to calculate system performance. The scale of the sensed image was then allowed to exceed the design limits of the system to find the effect on the correlation peak. The correlation coefficient and the shape of the correlation peak were used as figures of merit to judge the success of each trial.

This study applies the theory of Mellin-Fourier correlation to imagery collected by a sensor carried aboard a helicopter. The correlator modeled here is intended to represent an optical implementation of a scale invariant

system. Such an optical signal processing system can be modeled realistically by numerical experiments. The limited dynamic range of optical systems is simulated by scaling all imagery amplitudes between 0 and 255 each time a transformation is performed. The response to high noise levels is used to evaluate the immunity to background clutter. Trials conducted with real sensed imagery provide a realistic test for a scale invariant pattern recognition system intended for tactical applications. These trials show that the scale and rotation invariance predicted by theory can be applied in practice. The space bandwidth of the correlator is varied, and the effects on the correlation images suggest design approaches for equipment using Mellin-Fourier principles.

Experimental techniques for both zooming and downsampling the reference image are developed to be able to provide a sensed image of exactly the proper scale and orientation for Mellin-Fourier correlation. In this way, the Mellin-Fourier correlator is evaluated with respect to small scale differences in the input. The effect of different amplitude distributions of added noise is noted on the peak value and shape of the correlation image.

The Mellin-Fourier image correlation process is two-dimensional in nature, but insight into the $\ln(R),\theta$ mapping operation and the correlation energy distribution is gained when results are presented in the form of one-dimensional plots. In this research, photographs taken from the television monitor of an image processing computer are used to portray the nature of the entire Mellin-Fourier process, but one-dimensional plots are used to show details of the energy distribution in the correlation image. Images are characterized by a plot of the intensity values along a line passing through the peak value of the image.

Additional experimental techniques, such as range adaptive bandpass, are applied to extend the normal scale invariance of the Mellin-Fourier type correlator. Anderson and Callary (4) calculated only the value of the correlation peak as a figure of merit for the Mellin-Fourier correlator. This investigation calculates the entire correlation image plane. Using this technique, the advantages of spatial filtering are made clear.

CHAPTER II
BACKGROUND

In the course of this investigation, it was recognized that use of the Mellin-Fourier correlation principle would require careful application of the Discrete Fourier Transform (DFT). The paragraphs that follow discuss several aspects of the DFT and show how to properly apply it to evaluate a pattern recognition system.

Experimental Techniques

Methods Used to Calculate Accurate DFTs

As mentioned earlier, in a pattern recognition system which uses transform techniques to achieve invariance to translation, scale, and rotation, the Fourier transform is usually used initially to provide translation invariance. Actual pattern recognition is performed on the magnitude of the Fourier transform of an object rather than the object itself. When the Fourier transform is computed, the spectral resolution achieved may be insufficient for reliable pattern recognition even though the Nyquist criteria have been met. The two issues of spectral resolution and Nyquist sampling must be considered separately.

In a DFT algorithm, the input record consists of N data points, each point representing T units, producing a record length NT units long. The output of the DFT algorithm will also contain N data points, each point representing a spatial frequency interval

delta f = 1/NT

The discrete frequency spectrum is repeated periodically at integer multiples of the sampling frequency $f_s = 1/T$, with the magnitude of the spectrum being symmetric about the folding frequency

f = (N/2) delta f = 1/2T

This folding frequency is a direct result of sampling the input signal, and gives rise to the Nyquist requirement of sampling at twice the highest spatial frequency present in the input signal. If sampling is done at less than the Nyquist rate, an effect called aliasing causes inaccuracies in the computed spectrum.

The DFT of an input record may be calculated with a resolution of delta f even though the Nyquist condition has not been met. However, the values computed for the spectrum will not be accurate because of aliasing, and any further use for pattern recognition may produce misleading results.

Alternatively, the number of data points, N, may be so small that the widely spaced samples do not completely describe the shape of the spectral curve, even though the Nyquist condition has been met and the samples are numerically accurate.

Thus, two considerations apply to all invariant pattern recognition schemes which use digital transform techniques:

1. Spectral resolution must be sufficient to show identifying features of the pattern.
2. Nyquist conditions must be met to assure numerical accuracy of spectral samples.

Windowing and Truncation

Practical application of the principles above involves data windowing and truncation. These two effects are manifest in the spatial domain and spatial frequency domain, respectively. Windowing of input data must be performed to minimize the effects on the Fourier transform of a finite input record length. The DFT produces an output that is always a combination of the actual data spectrum and the window spectrum (6). The window is usually a rectangular function of unity amplitude which is multiplied by the data. The DFT results in the convolution of the spectrum of the window with the spectrum from the pattern of interest.

the DFT is periodic, Nyquist conditions require that the highest spatial frequency present in a record of N samples be N/2 cycles per frame. The abrupt transitions at the edges of a rectangular window cause very high spatial frequencies to occur in the spectrum. These spectral components can be significant at N/2 cycles and can cause aliasing errors to occur. One way to reduce the components at N/2 cycles is to make the edge transitions less abrupt by using one of the well known smoothing windows such as the Hamming, Hanning, or cosine functions. The need to condition all data with a window before computing the DFT stems directly from the Nyquist sampling condition. Proper windowing assures numerical accuracy of all Fourier transform samples computed using the DFT (6). The window used in this research tapered all images to 1/2 the original value at each edge, reducing the frequency components at the edge of the Fourier transform plane.

In a way completely analogous to windowing, truncation of Fourier transform records avoids errors in computing the cross correlation of two functions. In one dimension, the cross correlation of two records of length N results in 2N valid data points. If transform techniques are used to perform the cross correlation, each Fourier transform computed must be truncated to one-half its original size before multiplication and inverse transforming. Otherwise,

an effect called cyclic correlation causes errors in the cross correlation plane (7). This effect is similar to aliasing, but occurs in the cross correlation domain instead of the spatial frequency domain.

Considerations for Geometric Transformations

The spatial frequency characteristics of the Fourier transform magnitude of the input pattern must be considered if system space bandwidth is to be used most effectively. The symmetry of the Fourier transform magnitude may be used to reduce space bandwidth requirements by taking all samples from the upper half plane of the diffraction pattern. The upper half plane of the diffraction pattern contains all of the recoverable shape information about an object, even though position information is lost. All available space bandwidth (sampling capability) should be devoted to this region when the geometric transformation is done. Only a portion of the Fourier transform plane carries relevant shape information, and a geometric transformation that adapts to that frequency band and devotes full resolution to the most relevant spatial frequencies is most likely to provide the discrimination desired. In this way, invariance to scale may be extended to cover more than the range obtained with a transformation which maps over a fixed frequency band.

Previous investigators have designed the polar transformation to operate over a fixed spatial bandpass in the Fourier transform plane, thereby limiting the inherent scale invariance of the geometrical transform (8). Since size information about the expected object is often available, it may be used to select the most appropriate area in the Fourier transform plane and thereby extend the normal scale invariance of the Mellin-Fourier correlator.

Choosing a Figure of Merit

In evaluating a Mellin-Fourier correlator, a figure of merit must be used which reflects the pattern recognition ability of the system. Experimental considerations such as the tendency of many sensors to drift or change the average value of an image over time may cause the cross correlation peak value to decrease even though the pattern match with a reference image is nearly perfect. In cases where the spatial frequency filter in the correlation plane includes the center, or d.c., point, the correlation coefficient

should be normalized to the energy in the reference image using the expression

$$C(X,Y) = \frac{\int [S(X',Y') \cdot R(X+X',Y+Y')]dX'dY'}{[\int [S(X',Y')]^2 dX'dY' \cdot \int [R(X',Y')]^2 dX'dY']]^{1/2}}$$

where

$C(X,Y)$ = correlation image plane

$R(X,Y)$ = reference image

$S(X,Y)$ = sensed image

X',Y' = coordinates used as dummy variables in computing the cross correlation

This expression was used for calculation of the correlation coefficient throughout this work.

Theory for Extending the Normal Scale Invariance

Use of the Mellin transform for pattern recognition would seem to require more space bandwidth, i.e., more samples, than required to obtain the original reference pattern. A brief analysis of the resampling process will show how the requirements for increased space bandwidth may be minimized.

The theory developed to make full use of sampling capability is best illustrated by an example in one dimension. Figure 3 shows the relationship between sample spacing in the Fourier transform plane, designated as X space, and sample spacing in the ln (R),θ plane, designated

as X' space. The samples in X' space occur at equally spaced intervals of the variable X'. The coordinate transformation that achieves scale invariance is represented by a curve that follows the functional form

$$X'_k = \ln (X_k / X_{min})$$

where

X_k = k^{th} sample in X space

X'_k = k^{th} sample in X' space

X_{min} = minimum value of spatial frequencies in Fourier plane

The sampling in the Fourier transform plane extends over an interval between X_{max} and X_{min}, and the samples have a non-uniform spacing along the X axis. The widest spacing in X occurs at X_{max} and the closest spacing occurs at X_{min}. Since the sample spacing in X is most dense at X_{min}, it is best to assure that this part of the sampling curve has samples in X that are as far apart as possible if the system bandwidth is to be most effectively used. At the same time, the interval at X_{max} must be no greater than the Nyquist distance in order to preserve all the information present in the original image. The slope of the logarithmic curve at X_{max} is determined by the Nyquist requirement, and the space bandwidth of X' space is largely determined by the slope of the sampling curve at X_{min}.

When Mellin-Fourier correlation is done in two dimensions, the X' axis in Figure 3 represents the ln(R) axis in the ln(R),θ plane. The X axis represents the radial frequency coordinate, or R, in the Fourier transform plane. If the chosen region in the Fourier transform plane does not change position and adapt to the new object spatial frequencies as the object scale changes, information may enter or leave the annulus defined by earlier size estimates. The new information appearing in the ln (R), θ image will cause the cross correlation with a reference pattern to be reduced. To prevent the reduction of the cross correlation peak, the chosen region in the Fourier transform plane must adapt by changing position when a scale change occurs in the object. Specifically, system space bandwidth may be conserved by using range adaptation in two ways:

(1) using expected object range to select the annulus of spatial frequencies in the Fourier transform plane over which resampling will be done

and

(2) using the analysis developed for minimizing the slope of the resampling curve at X_{min} to modify the transformation equations to map the spatial frequency annulus into the full space bandwidth of the ln(R),θ plane.

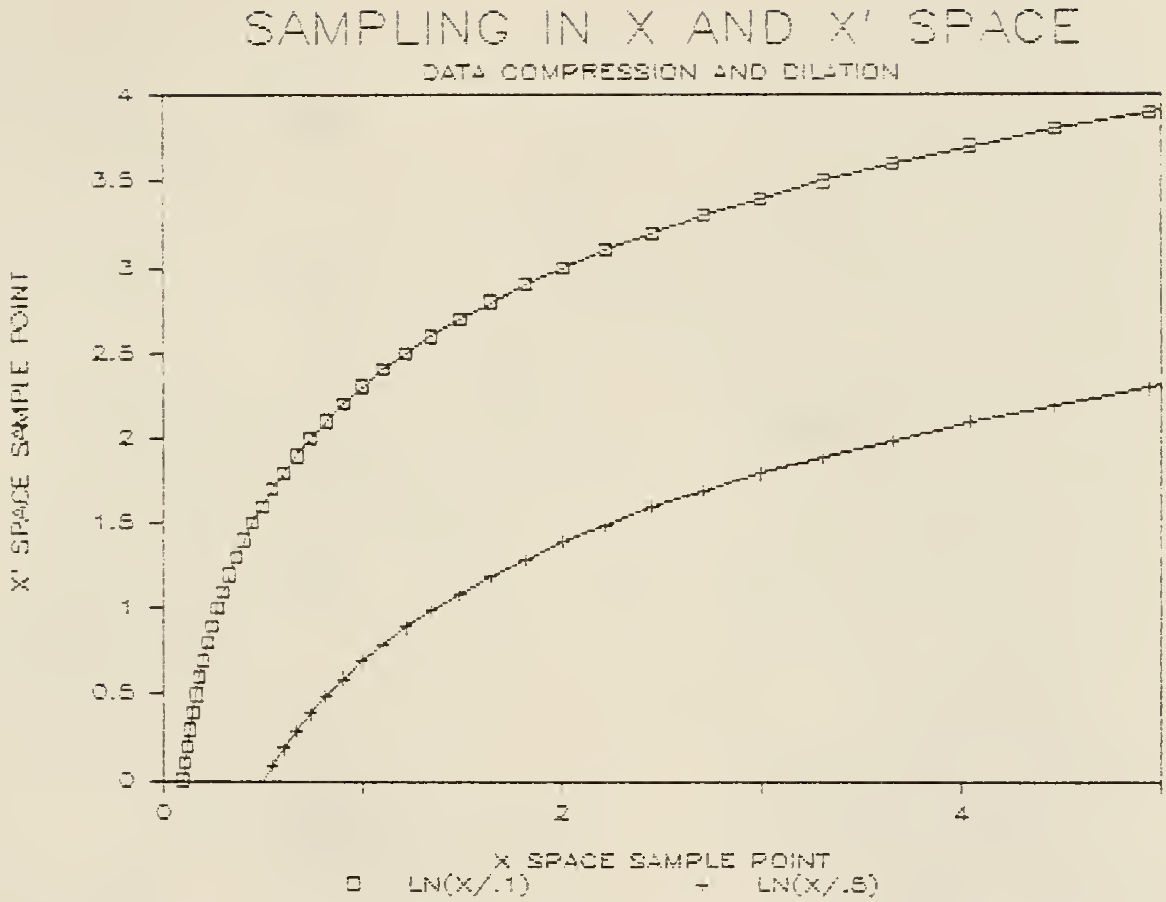

Figure 3. Sample spacing in the Fourier transform plane, X space, and in the ln(R),θ plane, X' space.

These steps will assure Nyquist sampling over the chosen region in the Fourier transform plane, and will minimize oversampling at the smallest value of the input coordinate.

Adapting The Coordinate Transformation

The upper curve in Figure 3 represents sampling done using a fixed set of transformation equations in which X_{min} = .10. The lower curve represents sampling done with an adaptive tranformation equation with X_{min} = .50. If the relevant information remains within a fixed domain when a scale change occurs, and only translates, the lower curve shows that sampling requirements in X space are less severe, i.e., samples are further apart, than if the transformation equations are left fixed and the upper curve is used to generate sample coordinates in X space. The number of samples in X' space necessary to meet the Nyquist conditions in X and still keep oversampling to a minimum at X_{min} determines the space bandwidth requirements of the scale invariant correlation system. The theory developed by Anderson and Callary makes use of the assumption that no information is allowed to leave the interval between X_{min} and X_{max} when a scale change occurs (9). This means that there are no "accuracy" problems such as the ones in the analysis of Cassasent and Psaltis (10). This is the basis for the savings in space bandwidth claimed in Reference 9.

Sample Adaptive Calulation

An example will show how range adaptation may be applied to a specific pattern to derive a spatial frequency filter for use in a Mellin-Fourier correlation scheme. The filter is a window applied to the Fourier transform plane, defining the area to be resampled. The width and boundary values of the region are determined by the nature of the object to be recognized and the expected range at which it will be encountered. In the Fourier plane, the filter specification will be two radial values determined from calculations of expected object size in the sensor field of view. The resampling scheme will then be applied to the region to minimize oversampling in the Mellin-Fourier correlation. For this example, it is assumed that other sensors have provided approximate range as R meters, and that the image and Fourier transform are made up of N x N arrays. If the sensor field of view is F degrees, then the number of pixels, P, occupied by a feature of size S is

$$P = (NS) / (R \tan (F))$$

In a reference image, a square feature of size P produces a first spectral lobe which goes to zero at N/P pixels from the center pixel in the Fourier plane. The first zero crossing defines a boundary value for the region chosen for resampling. Two boundaries of the spatial frequency bandpass may be established from estimated object feature

sizes in the image plane. The two cutoff frequencies will then define an annulus of spatial bandpass in the Fourier transform plane. For a sensor with a field of view of 3 degrees, the cutoff frequencies for a 6 meter object with .5 meter features at a range of 500 meters are

$$\text{upper frequency} = N/P = (R \tan(F))/S$$
$$= (500/.5) \tan (3)$$
$$= 52 \text{ cycles/frame}$$

$$\text{lower frequency} = (500/6) \tan (3)$$
$$= 4 \text{ cycles/frame}$$

The full space bandwidth of the Mellin-Fourier correlation resampling system may then be applied to an annulus between 4 and 52 pixels from the center or d.c. term in the Fourier transform plane. The transformation equation necessary for optimal resampling may be written in terms of radial distances in the Fourier transform plane:

$$R' = \ln(R) - \ln(R_{min})$$

where

$$R_{min} < R < R_{max}$$

This equation is used to generate sample coordinates in the $\ln(R),\theta$ plane where the value of R_{min} is the lower spatial frequency limit derived for the specific pattern, 4 pixels, and the value of R extends to the upper frequency limit, R_{max}, of 52 pixels. The region in the Fourier plane that is oversampled to construct the logarithmic data record does

not begin until a radius of 4 pixels has been reached in the Fourier plane, thereby minimizing the oversampling that occurs at small values of the Fourier radial coordinate. Since no data of interest lie beyond a radius of 52 pixels in the Fourier plane, the sampling that occurs at 52 pixels from the center can be made to just meet the Nyquist rate.

The analysis above has shown how system space bandwidth may be conserved by using range adaptation to define the proper annulus in the Fourier plane and then adapting the transformation equations to map the annulus into the $\ln(R),\theta$ plane. When range adaptation is performed as a normal part of signal processing, like proper windowing, the space bandwidth requirements of a pattern recognition system may be expressed in terms of spectral resolution in the Fourier plane rather than sampling bandwidth in the $\ln(R),\theta$ plane. It may be argued that knowledge of range for the sensed image would allow the sensed Fourier transform to be scaled appropriately, thus making scale invariant schemes unnecessary. In a practical system, however, range information is usually only approximate, making the sensed frequency annulus poorly defined. Range adaptation is valuable because it makes a correlator more tolerant to errors in size estimates for the sensed image. Evidence of this tolerance is shown in the examples of the next chapter.

CHAPTER III
APPLYING OPTIMUM SAMPLING TECHNIQUES

Examples of Optimum Sampling

The Fourier transform patterns in Figures 4 and 5 have been generated to illustrate the technique of designing a transformation which maps the Fourier transform space into another space with coordinates R and θ. The patterns in Figures 4 and 5 represent the magnitude of the Fourier transform of squares of sizes 10 X 10 and 20 X 20, respectively. The Fourier transform image is represented by a plot of intensity along the center of the image. Figures 6 and 7 are from the R,θ mapped images. Study of the size of the features in Figures 6 and 7 shows that these features change size and position with the object scale change, just as they do in the Fourier transform image before mapping. In this case the scale change encountered is a factor of 2. Figures 8 and 9 are from the ln (R),θ mapped images. Here the features present in Figure 8 simply translate to a new position in Figure 9; they do not change size. However, new information is introduced from the right in Figure 9 which was not present in Figure 8. Distortion is also introduced in both figures because of the many-to-one mapping that occurs at small values of radial distance in the Fourier plane.

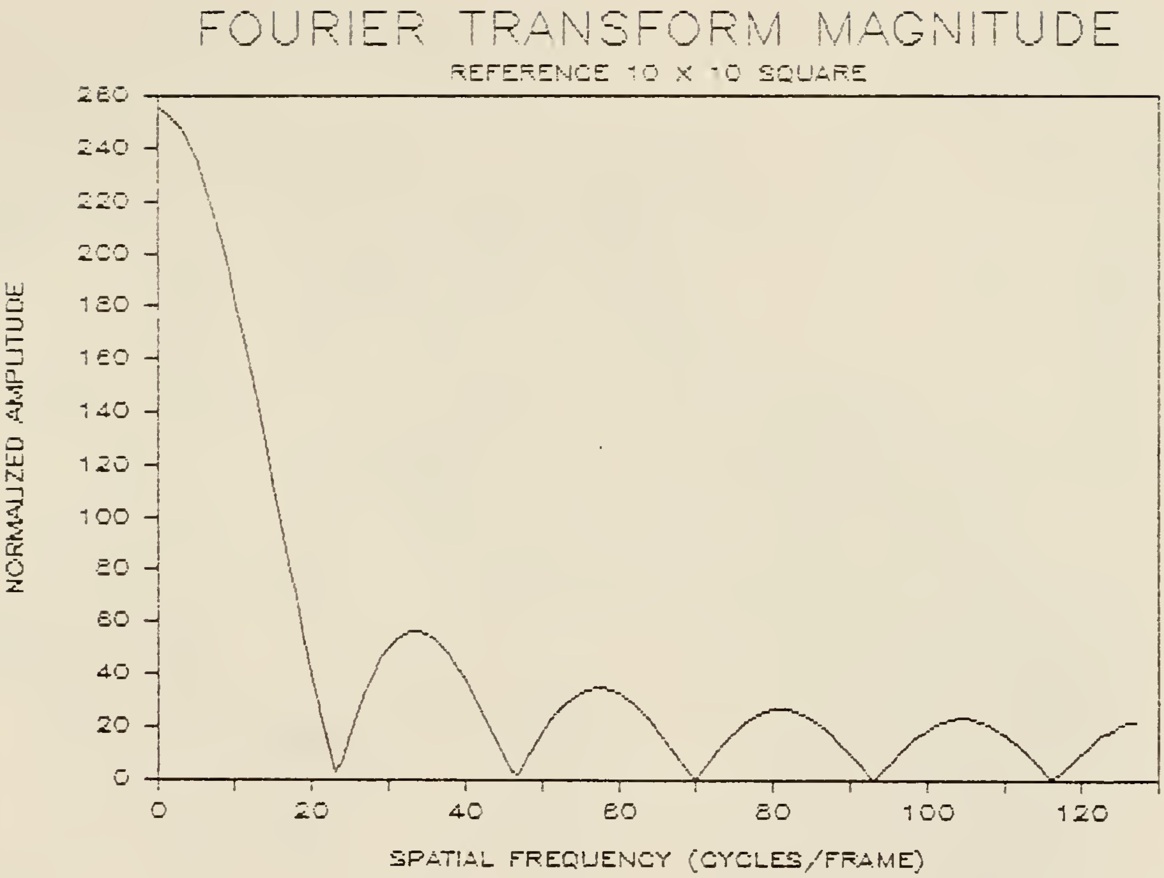

Figure 4. Amplitude along a line passing through the center of the Fourier transform of a 10 X 10 square. Normalized from 0 to 255.

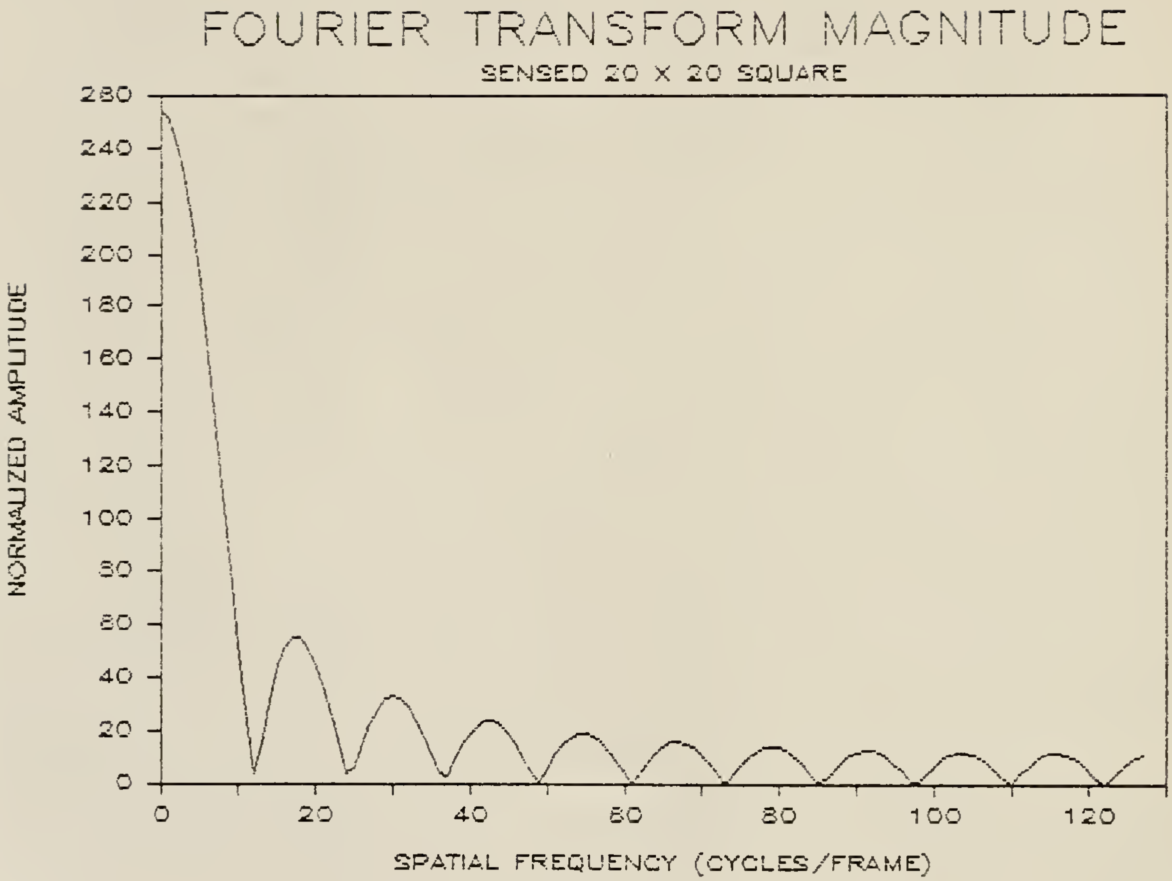

Figure 5. Amplitude along a line passing through the center of the Fourier transform of a 20 X 20 square. Normalized from 0 to 255.

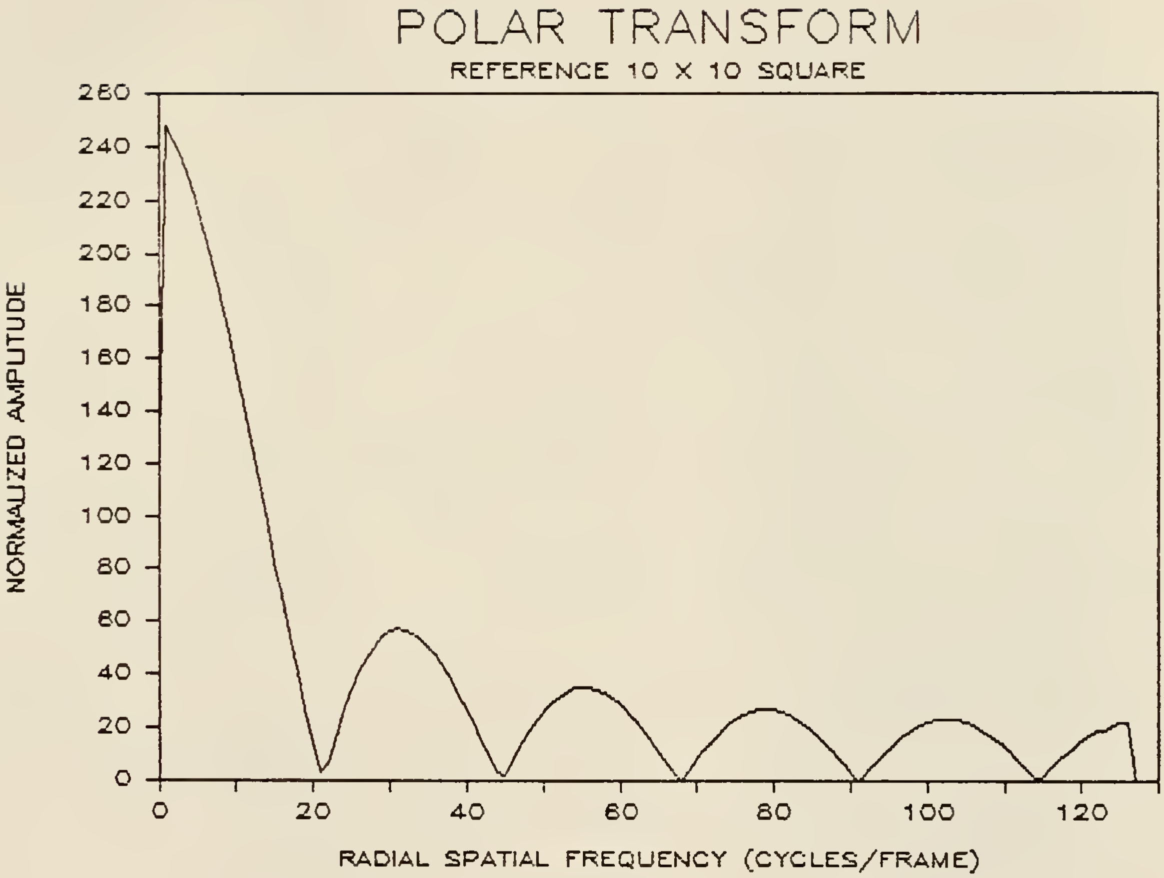

Figure 6. Amplitude along a line passing through the center of the R,θ mapped image if a 10 X 10 square. Normalized from 0 to 255.

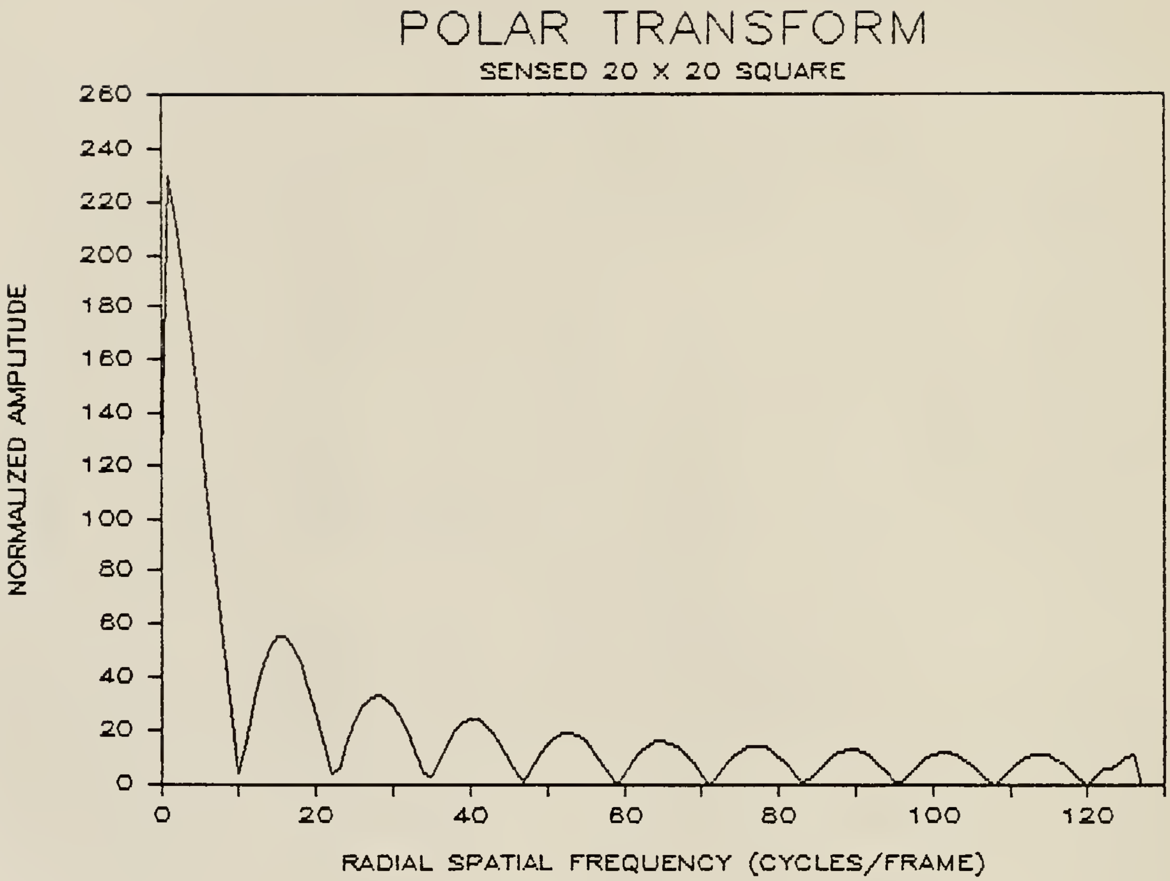

Figure 7. Amplitude along a line passing through the center of the R,θ mapped image of a 20 X 20 square. Normalized from 0 to 255.

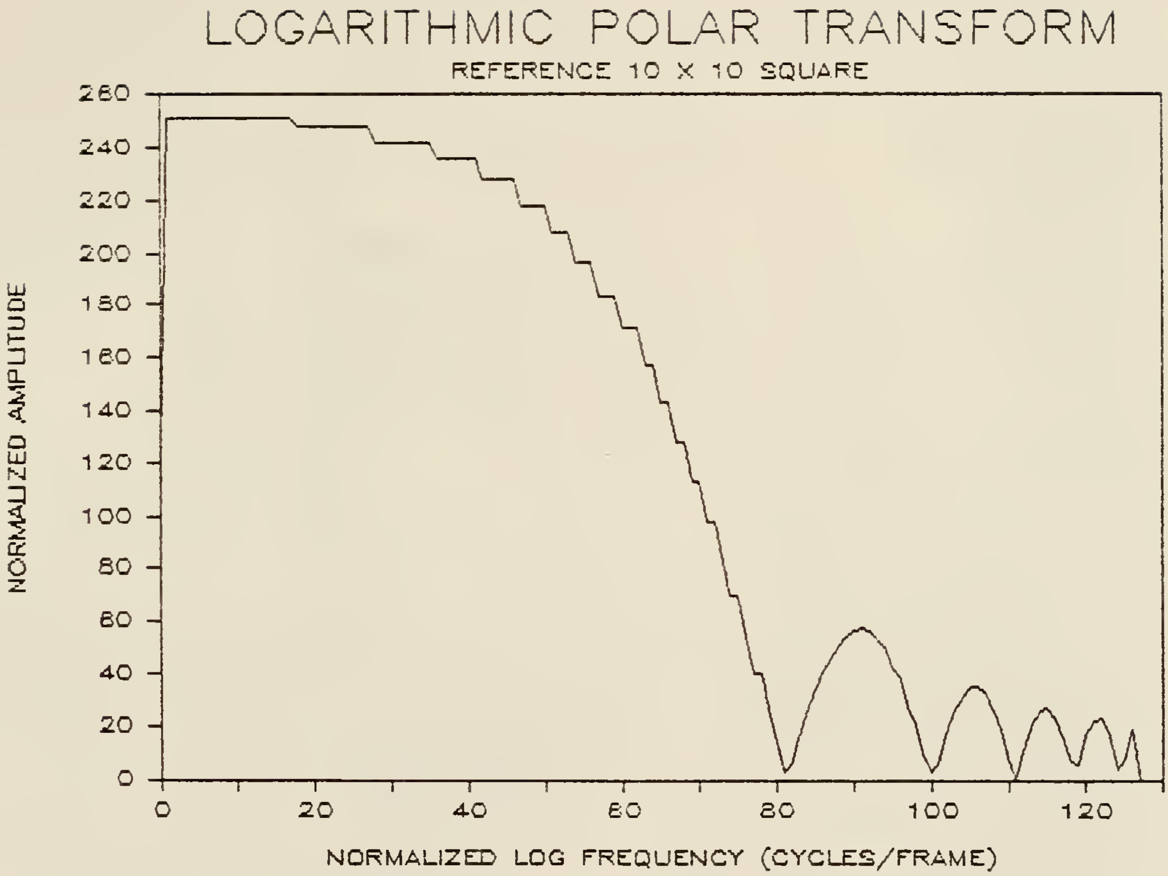

Figure 8. Amplitude along a line passing through the center of ln(R),θ mapped image of a 10 X 10 square. Normalized from 0 to 255.

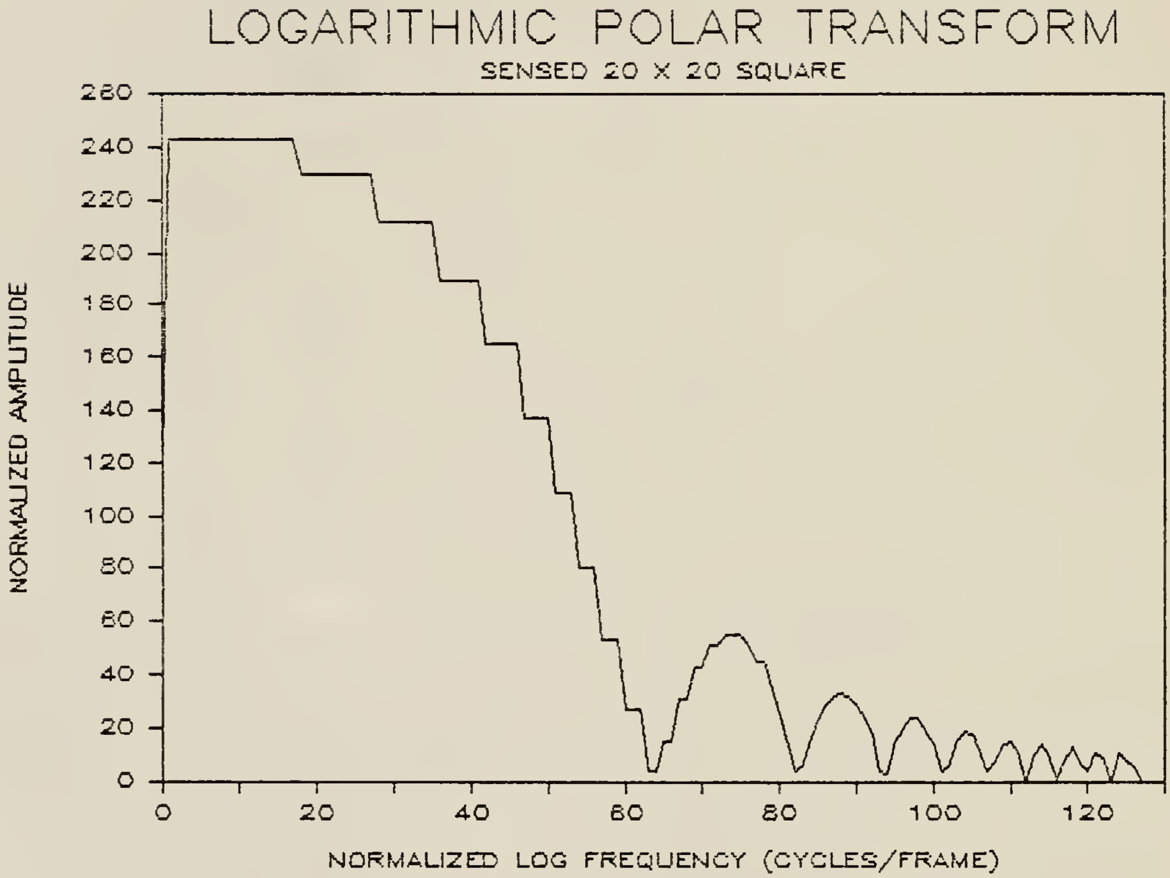

Figure 9. Amplitude along a line passing through the center of the ln(R),θ mapped image of a 20 X 20 square. Normalized from 0 to 255.

In producing both Figure 8 and Figure 9, the same transformation parameters were used; i.e., the mapping was governed by the same set of equations. For each figure, pixel values in the ln (R),θ space were derived from the same calculated position in the Fourier transform space. With a fixed set of transformation equations, a scale change causes new information to enter the transformed image, causing a decrease in the cross correlation peak value. This difficulty may be overcome by adapting the transformation equations to map a different region of the Fourier transform plane into the new space. In Figures 8 and 9, range information was used to choose the size and position of the annulus in the Fourier transform plane, and the annulus tracked the region of critical object information over a wider range of scale change. Of course, spatial resolution in the transformed image will degrade as the annulus chosen for the transformation becomes smaller and smaller. This occurs at very close ranges, and is not critical if the reference image is made at the closest expected range. In a system with the ability for range adaptive bandpass, range information is used to change the transformation parameters to track the critical region of spatial frequencies in the Fourier transform plane. The cross correlation peak should remain high over a wider range

of scale change than when the peak is reduced due to scale changes causing irrelevant information to enter the transformed space.

Figures 10 through 13 show the results when the principles discussed above are applied to real images. The sequence of nine images that make up each figure show the Mellin-Fourier correlation process outlined schematically in Figure 1. The upper left pair of images labeled "REFERENCE" and "SENSED" are infrared images of an armored vehicle. The right image of the pair has been rotated about its center by 45 degrees. The second pair of images labeled "REFERENCE FFT" and "SENSED FFT" are the magnitudes of the Fourier transforms. The image pair labeled "LOG R, THETA TRANSFORMS" are the $\ln(R),\theta$ mappings done from the Fourier transform images immediately above. The right $\ln(R),\theta$ image shows that rotation in the sensed image produces vertical translation of the pattern in the $\ln(R),\theta$ image. The images labeled "MELLIN TRANSFORMS" are the magnitudes of the Fourier transforms of the images immediately above. Since the only difference between the reference and sensed $\ln(R),\theta$ images is a vertical shift, the magnitude images labeled "MELLIN TRANSFORMS" are nearly identical. The last step in the Mellin-Fourier correlation process is shown as the rightmost image labeled "CROSS CORRELATION." The real and imaginary components of the $\ln(R),\theta$ images were used to compute the cross correlation image plane. The dark spot in

Figure 10. Sequence of images showing the Mellin-Fourier correlation process. The sensed image has no scale change, but is rotated by 45°.


EFFECT OF ROTATION
REFERENCE
SENSED
ROTATION OF 45 DEGREES
REFERENCE FFT
SENSED FFT
CROSS CORRELATION
(PEAK AT 45 DEGREES)
LOG(R), THETA TRANSFORMS
MELLIN TRANSFORMS

Figure 11. Sensed image scaled by a factor A = 2.0 with no rotation.

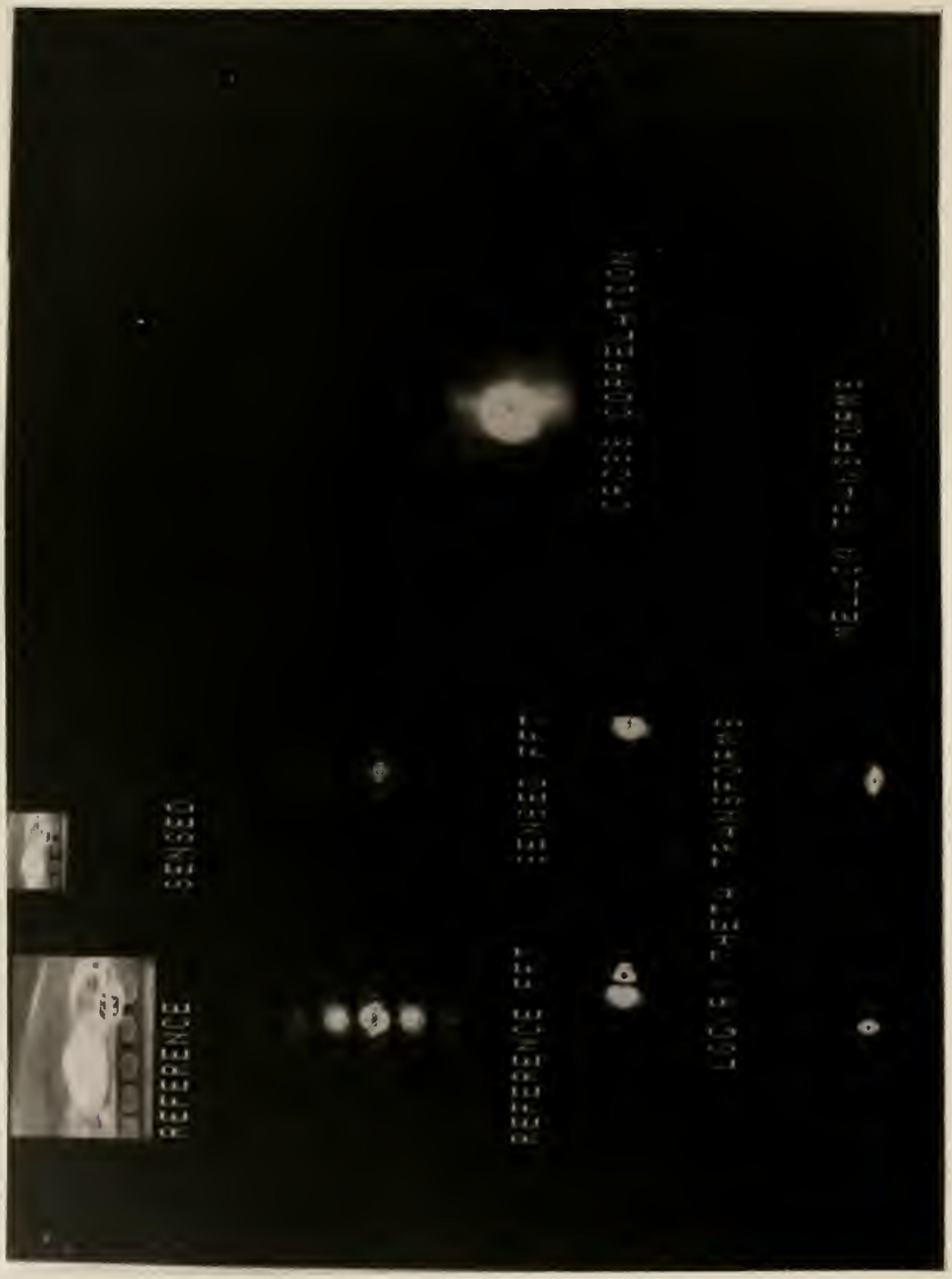
REFERENCE
SENSED
REFERENCE FFT
CROSS CORRELATION

Figure 12. Sensed image scaled by a factor $A = 2.0$ with $45°$ rotation.

Figure 13. Sensed image scaled and rotated. Range adaptation used to restore the value of the cross correlation peak.


REFERENCE
SENSED
REFERENCE FFT
SENSED FFT
CROSS CORRELATION
LOG(R)-THETA TRANSFORMS
MELLIN TRANSFORMS

the correlation image is enhancement performed by the image processing computer to make the peak in the correlation plane more visible. The vertical position of the correlation peak reveals the correct rotation difference between the reference and sensed images, i.e., 45 degrees, and the amplitude, indicated by the peak intensity, shows the degree of similarity between the reference and sensed images.

Figure 10 shows that rotation of the input image by 45 degrees may be detected using standard space variant processing techniques. In this example, no scale change was involved, and pattern recognition was achieved with a normalized correlation coefficient of .9. In Figure 11, the sensed image was scaled by a factor of 2.0, and no rotation was present. The images labeled "LOG (R), THETA TRANSFORMS" show what happens when a scale change causes information to leave the ln (R),θ plane. The correlation coefficient is reduced to .7, even though its position is displaced from the center of the correlation plane by the correct amount, indicating a scale change. Figure 12 shows that combining a scale change with a rotation reduces the correlation coefficient still further to .6, with the appearance of noise at high spatial frequencies being evident in the ln (R),θ images. Application of range

adaptive bandpass in Figure 13 restores the correlation coefficient to .89, with the rotation being correctly sensed. However the ability to detect the amount of scale change by the position of the correlation peak has been given up by adapting the ln (R),θ transform equations using range information from an independent source.

Testing Theoretical Predictions

Predicted Scaling Limits

The success of the application of Mellin-Fourier correlation to the tactical images shown in Figures 10 through 13 led to a careful analysis of the scale invariance that should be expected of the Mellin-Fourier correlator when used with a particular image frame size. The images used in predicting the expected scale invariance were centered in a frame of 256 X 256 and were scaled by sampling in a polar coordinate system in which R was multiplied by a scaling constant A. The value of A was used as an index to denote the amount of scaling present in each trial. An image of the Fourier transform of the reference scene, a side view of an armored vehicle, was inspected to identify the most critical features for pattern recognition. The selection of "most critical" features in the Fourier transform plane was subjective to the extent that some spatial frequencies were identified with the reference image window and were eliminated by specifying the lower limit of

the filter. Also, knowledge of imager characteristics as well as inspection of large numbers of Fourier transform images allowed an upper limit to be specified for the spatial bandpass. Limiting the frequencies used for transformation into the $\ln(R),\theta$ plane allowed the frequencies to be adjusted for the scale change present in the sensed image. The adaptation of the filter according to scale change is a capability that is often present in tactical pattern recognition systems with radar altimeters or laser rangers.

Calculations were done using the side view of the armored vehicle as a reference image to verify that the distinct features in the Fourier transform plane were due to the spacing and number of the vehicle road wheels. The window or frame size of the reference image was used to calculate the location of the first zero crossing in the Fourier transform plane. These calculations were patterned after the example given in Chapter II, under "Sample Adaptive Calculation." The filter limits calculated using the methods described above resulted in an annulus in the Fourier transform plane between 20 and 110 pixels. For range adaptation, the lower and upper limits of this annulus were scaled according to the factor A used for the sensed image. The inverse relationship between scaling in the image plane and scaling in the Fourier transform plane

caused the filter boundaries to be multiplied by 1/A whenever the sensed image was scaled by A. The convention used in this research was that values of A greater than 1.0 resulted in a smaller image but a larger Fourier transform. Values of A less than 1.0 denoted a larger image and a smaller Fourier transform.

The scaling limits predicted for the example discussed above were determined from Nyquist sampling and spectral resolution requirements. It was observed from inspection of the Fourier transform of the reference image that this imagery was not corrupted by aliasing effects, and that the lower frequency limit of 20 pixels still provided an adequate number of samples to define a spectral lobe when scaling by a factor of A=.3 was performed. When scaling by factors larger than A=1.5, it was observed that loss of high frequency information pertaining to road wheel spacing, e.g., the second lobe moving out of the sampled domain, would violate the Nyquist condition. Therefore the predicted range of scale invariance for the correlator chosen for this example was from A=.3 to A=1.5.

Figure 14 shows the results obtained using the computer simulation of the Mellin-Fourier correlator. The points labeled with a square symbol were obtained from a correlator with the spatial filter fixed at 20 to 110 pixels. The

filter did not adapt to scale changes in the sensed image. The correlation coefficient steadily decreases from .9 with no scale change, and drops below the threshold of .7 if A is less than .5. The points labeled with cross symbols were obtained from a correlator in which the spatial filter adapted to the scale change present in the sensed image.

The annulus defined in the Fourier transform plane for the ln (R),θ transformation was allowed to change size according to the scaling factor A. This adaptation of the spatial filter allowed the correlation coefficient to remain fairly constant over the entire range of predicted scale change. The correlation coefficient for the adaptive correlator does not drop below .7 until A becomes smaller than .1. This represents an extension of the scale invariance for small values of A by a factor of 5. The performance of the correlator when A was greater than 1.0 was similar for the fixed and for the adaptive filter. At A=1.2 the upper frequency limit of the adaptive filter moved to a value of 128, which was the edge of the available bandwidth. Since the filter could no longer adapt, the correlators behaved similarly. These results show that adaptive filtering may be used to extend the normal scale invariance of the Mellin-Fourier correlator to allow pattern matches with high confidence (high correlation coefficient) even when operating near the lower limits for the scaling factor A.

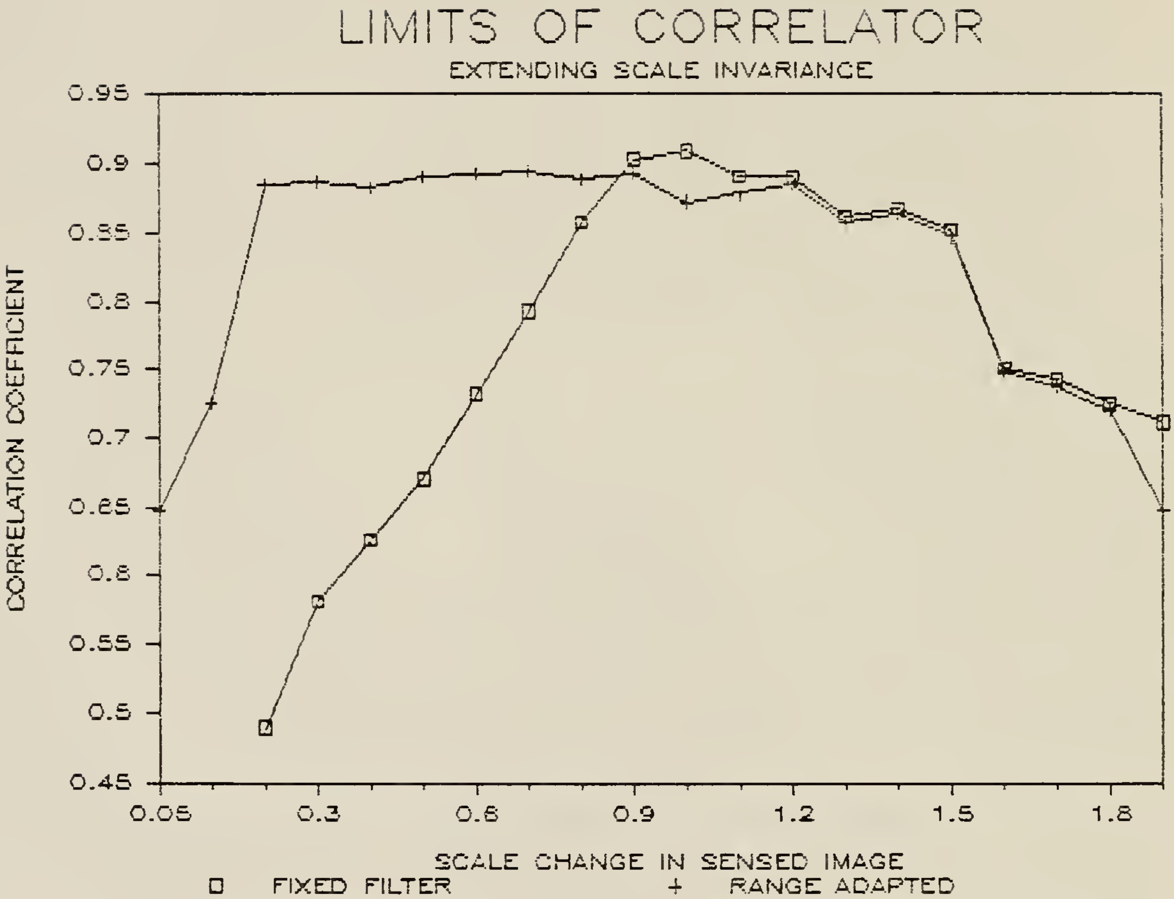

Figure 14. Scale invariance extended by adapting the spatial filter.

Failure Modes

Data acquired while investigating the scaling limits of the Mellin-Fourier correlator caused interest in information that could be obtained from the correlation plane even after the correlator had "failed" by giving a correlation coefficient less than .7. The position of the peak value in the correlation plane reveals the amount of scale change and rotation difference sensed, and this information seems to be reliable even when the value of the correlation peak is less than that required for a confident pattern match. Figure 15 is a plot of the scale change detected by the X position of the correlation peak versus the actual scale change present in the sensed image. As before, the square symbols show correlation done with a fixed filter, and the cross symbols show correlation done with an adaptive filter. The fixed filter gives incorrect values of scale change when the scaling factor A goes below .5, as predicted by sampling theory. The adaptive filter gives correct values of scale change (within 20%) when A=.05. The rotation reported by both correlators was within 10% of the correct value for the entire range of scale changes tested. With larger values of A, both correlators became insensitive to scale change, probably because the spectral features become larger and occupy more of the ln(R),θ plane, making small shifts in cross correlation harder to detect. This result suggests

that reliable indications of scale and rotation may be obtained from a Mellin-Fourier correlator using an adaptive filter even when the designed scale change has been exceeded. Correlator system design may be extended to cover values of scale change not allowed by sampling theory if information about scale change and rotation are required rather than the degree of pattern match.

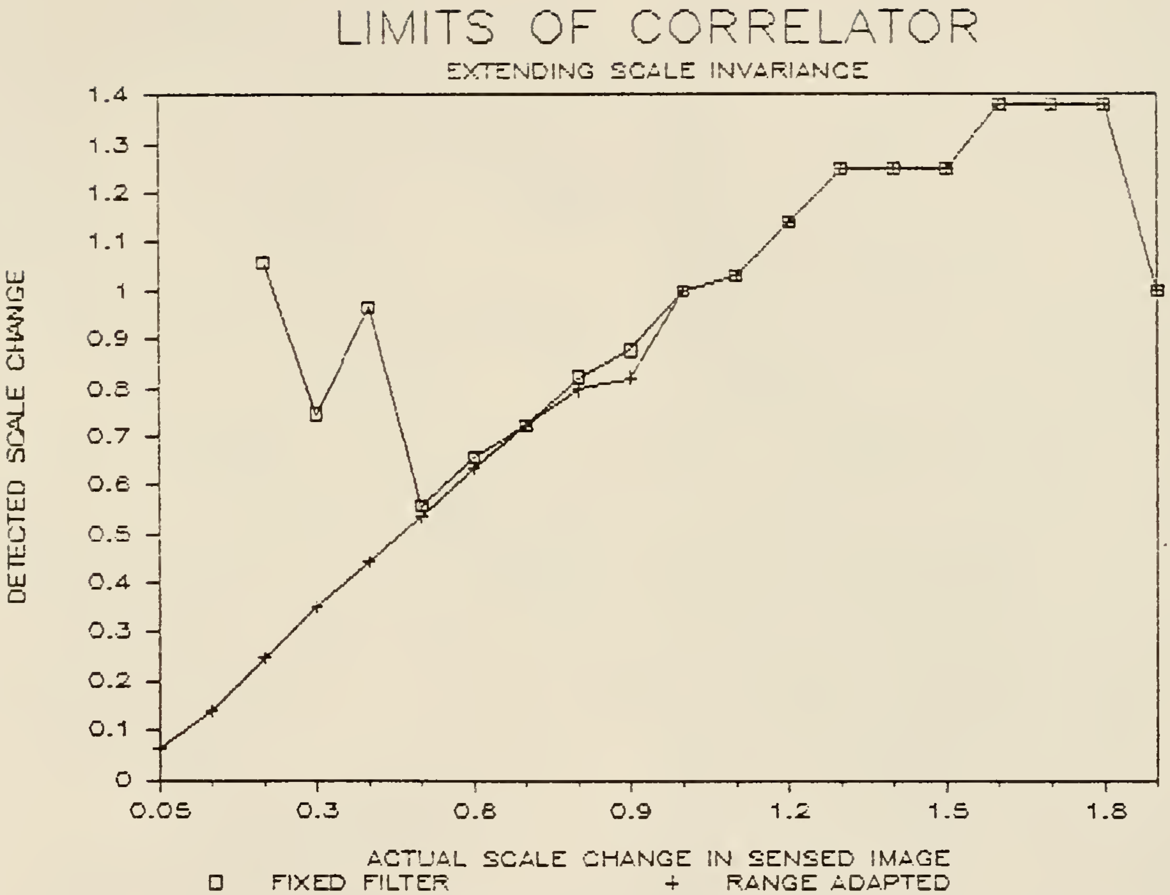

Figure 15. Detected scale change extended by adapting the spatial filter.

CHAPTER IV
ADDITIONAL EXPERIMENTS

Higher Space Bandwidth

The tests shown in Figures 10 through 13 were repeated with images having a space bandwidth of 256 X 256 pixels. The larger image format was equivalent to sampling the reference and sensed patterns at a higher frequency. To create the Fourier transform patterns, the 128 X 128 input images were simply centered in the 256 X 256 frames. No additional information was added to the input image, but the Fourier transform calculated over the 256 X 256 frame extended to higher spatial frequencies. This added space bandwidth allowed for more shift, i.e., more scale change, in the ln (R),θ images when scale changes caused distortions in the Fourier transform plane. The annulus of spatial frequencies chosen for logarithmic resampling was chosen using the same criteria suggested in discussions of the range adaptive technique; i.e., frequency boundaries were established using approximate ranges supplied with the test imagery.

Expected Benefits of Higher Space Bandwidth

The calculations of the upper and lower spatial frequencies critical for pattern recognition may be done without knowledge of the system space bandwidth available. With the larger format frames however, the spatial frequency boundaries could extend to larger distances, i.e., more pixels, from the center or d.c. term. With the larger space bandwidth available in a 256 X 256 format, it was expected that it would be possible to vary scale over a wider range while maintaining the value of the correlation coefficient. Scale change was performed using a sample and hold technique, with the sensed image remaining centered in the frame for all scale changes. The sample and hold technique was implemented using the same equations to generate sample points that were used to rotate the reference image. The sample coordinates for the sensed image had to be generated in polar form in order to add the required rotation angle. To generate a scaled image, the radial coordinate for the sample points was simply multiplied by a scaling factor A. The effect of this sampling scheme was to provide a sensed image that was scaled or zoomed around the center of the reference image as well as rotated by the desired angle. When higher space bandwidth was used in the experiment shown in Figure 12, with scaling and rotation present, the correlation peak value changed from .6 to .7. This increase

was not considered significant since the correlation value was so close to the threshold of .7 considered necessary for pattern match. The threshold value of .7 for pattern match was experimentally determined by correlation experiments between both geometric shapes and real objects. In these experiments, even dissimilar objects produced correlation coefficients of .6. When range adaptation of the transformation equations was performed as in Figure 13 but using the higher space bandwidth, the correlation coefficient changed from .89 (with the 128 x 128 frame) to .92. This slight increase was not considered significant, considering the price paid in a four-fold increase in the number of sample points required.

Effects of Exceeding the Correlator Design

A detailed study of the effect of scale change on the correlation peak value and curve shape was performed on the images with the higher space bandwidth. The rotation angle between the reference image and the sensed image was fixed at 45 degrees to be sure that the location of the correlation peak still revealed the correct rotation angle. Scale factors of the sensed image were varied between .5 and 2.0, and Figure 16 shows a plot of the values of the correlation images along a line passing through the peak value. The two curves with the legends "A = .5" and "A = 2.0" represent the extreme values over which the

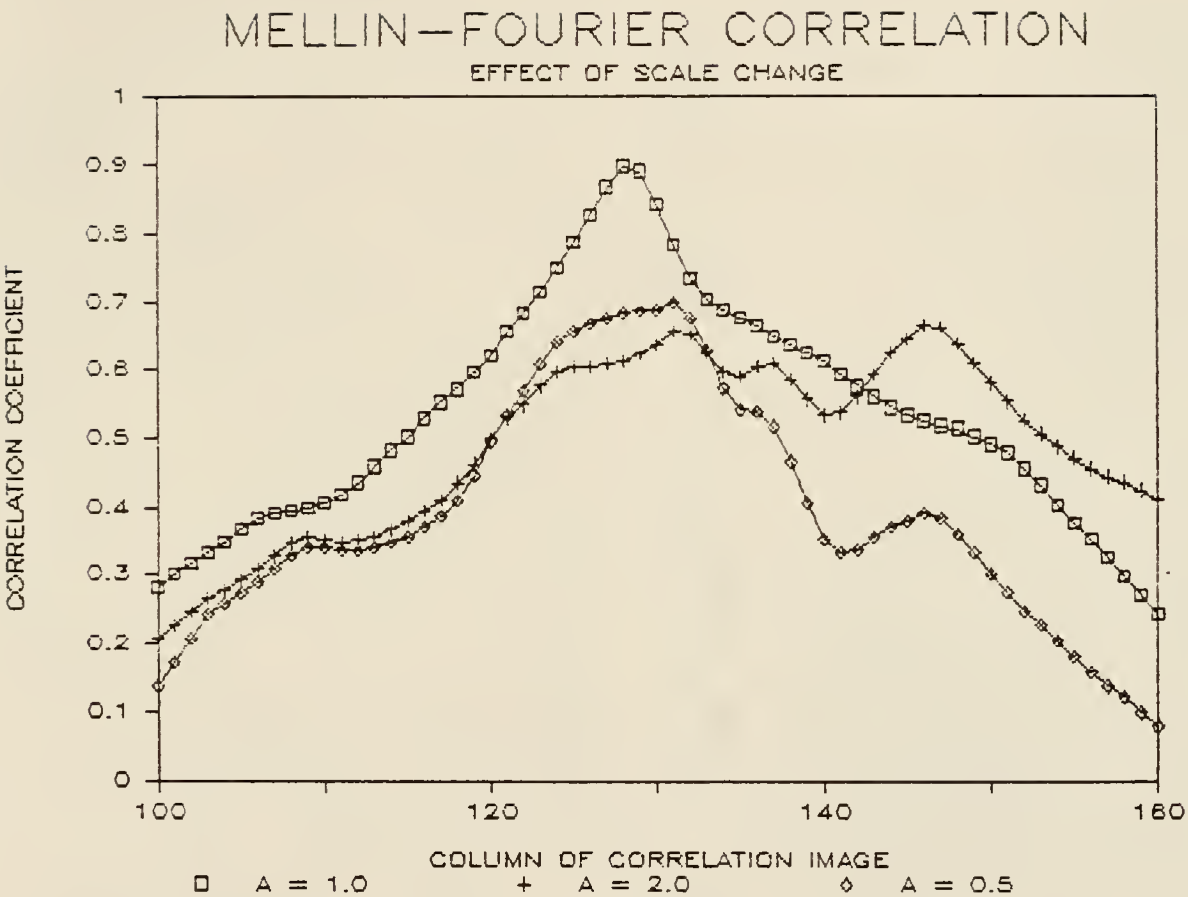

Figure 16. Shape of the correlation curve for two extreme values of scale change, A=.5 and A=2.0 . Range adaptive spatial filter not applied. The curve for A=1.0 represents a sensed image with no scale change.

Mellin-Fourier correlation scheme was exercised. The shape of the correlation curve for no scale change is shown in the curve labeled "A = 1.0." Symbols are included in the plots to define the curves when they cross each other.

The Mellin-Fourier correlator in this example was designed to cover a range of scale change from A = 2.0 to A = .5 without the use of range adaptive techniques. Figure 16 shows that the value of the correlation peak at these extreme scale changes drops just below the threshold value of .7. The range of scale change over which the system could operate in this example was not extended using range adaptive techniques. The use of higher space bandwidth has increased the range of scale invariance of the correlator only by the amount that was predicted from sampling theory.

Adding Noise

Effects of Adding Uniform Noise

A further investigation of the Mellin-Fourier correlation scheme was performed by adding noise to the sensed image and noting the effect on the shape and magnitude of the correlation peak. The intent of this part of the investigation was to simulate the imagery collected by a sensor that might be corrupted by various noise sources. The image used as a reference was the same as the

reference image in tests involving changes in scale and rotation, i.e., one which contained no added noise. A random variable function from a computer statistical library was used which was capable of generating a pseudo random number uniformly distributed between 0 and 1.0. The function is considered pseudo random because the seed, or initializing integer, completely determines the string of random digits generated by the function each time it is used. However, the probability distribution of the digits produced by the function is the desired uniform distribution. For initial investigations into the sensitivity of the Mellin-Fourier correlator to added noise, the sensed image was treated as a random variable to which another random variable with the desired statistical distribution was added. The addition of noise took the mathematical form

NOISY SENSED IMAGE = SENSED IMAGE + 255 X NOISE X RAN (SEED)

where

NOISE = value from 0 to 1.0 providing a measure of the amount of added noise

RAN (SEED) = random variable uniformly distributed from 0 to 1.0

The mathematical form above produced a sensed image with an altered amplitude distribution between values determined by the noise measuring variable NOISE. The total amplitude distribution of the sensed image was the combination of uniformly distributed noise and the original distribution.

The effect of varying the value of NOISE was to extend the area of the image histogram over which the added noise had its effect. One meaningful measure of this type of noise is the width of the histogram region that is altered. The degradation of the correlation peak when the sensed image was transformed by noise of uniform amplitude distribution is shown in Figure 17. As with the evaluations involving scale change, the correlation image was represented by a horizontal scan through the correlation peak. The three curves shown represent altered histogram widths of of 25, 50, and 128 counts; each region centered around the image mean value of 59 counts. Figure 17 shows that introduction of noise causes the cross correlation curve to decrease smoothly past the threshold amplitude considered necessary for pattern match.

Effect of Adding Gaussian Noise

A more physically significant Gaussian distribution was used in a second series of trials with the same sensed image. The Gaussian distribution was achieved by making use of the Central Limit theorem applied to the uniformly distributed random function described above. The mathematical form for the transformation was

$$Y = \sum_{K=1}^{K=48} \left[(\mathrm{RAN}(\mathrm{SEED}) - .5) / 2 \right]$$

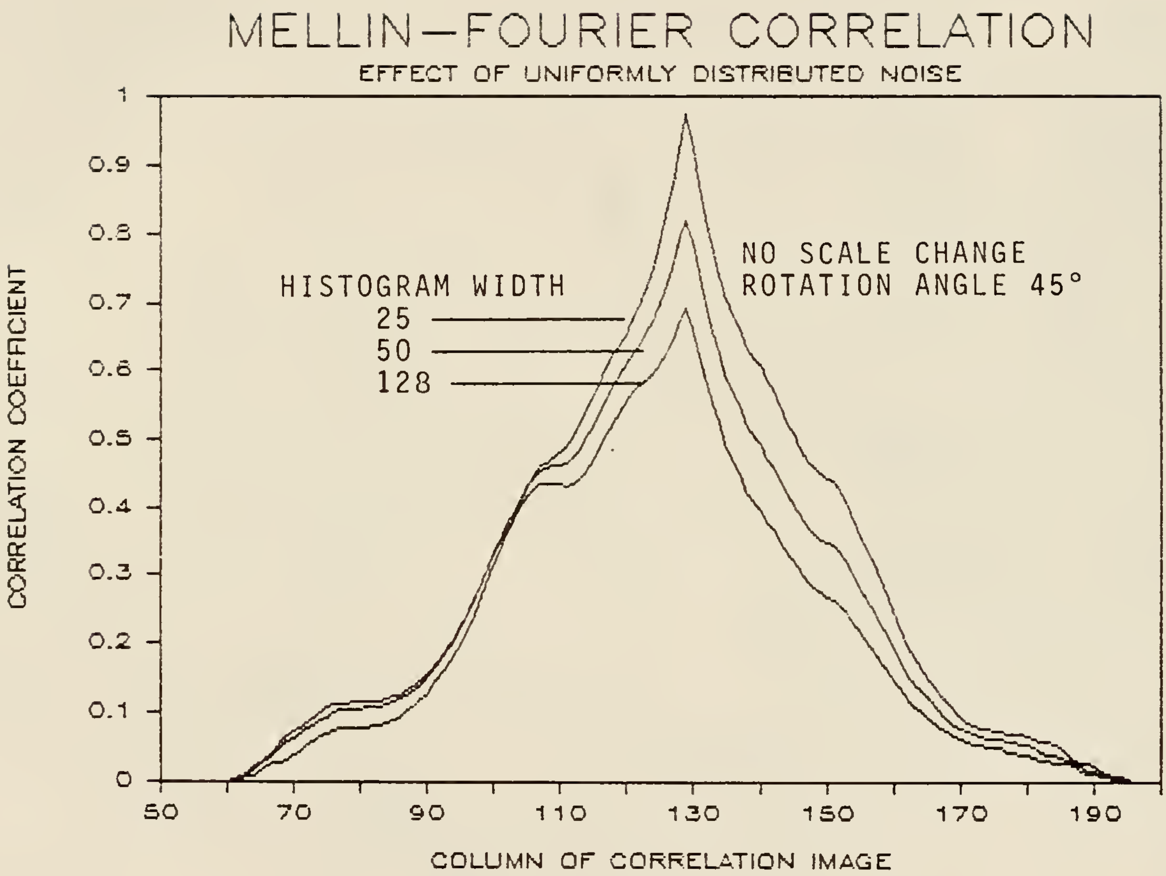

Figure 17. Uniformly distributed noise added to sensed image. Added noise was centered around the image mean value, and had the three histogram widths shown.

A new random variable, Y', with the desired mean of U and standard deviation V was obtained using the transformation

$$Y' = U + V * Y$$

The results of trials conducted with Gaussian distributed random noise are shown in Figure 18. The three curves represent the shape of the correlation curve after the addition of noise having standard deviations of 0, 10.0, and 20.0. The horizontal scale of Figure 18 was changed to see better that the correlation curve still has a discernible peak which is located at the proper scale and rotation coordinates even though the amplitude of the correlation peak has fallen below the threshold value of .7. This characteristic of the correlation image suggests that the ability of the Mellin-Fourier correlator to detect scale and rotation changes may be preserved even when noise levels have reduced the confidence in pattern matches between reference and sensed images.

Effect of Optimal Spatial Filter

During the course of the investigation into noise sensitivity, the spatial filter used to eliminate low frequencies in the Fourier transform plane was fixed for the reference and sensed images to pass all frequencies between radii of 10 and 128 pixels. The filter was not adapted to the scale change present in the sensed image. When the

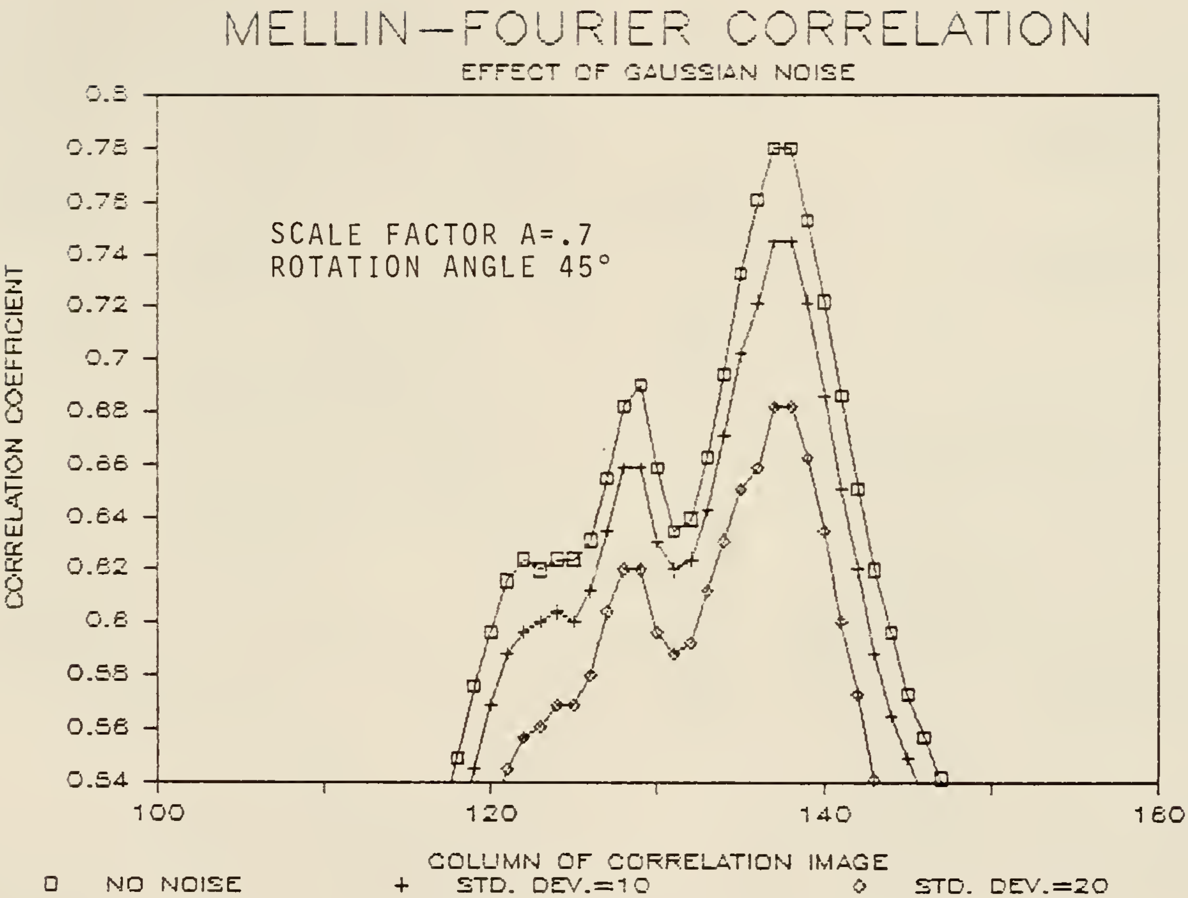

Figure 18. Gaussian distributed noise added to sensed image. Added noise was zero mean, with the three standard deviations shown.

sensed spatial filter was optimized for the scale change, Gaussian noise was again introduced into the sensed image to determine the effect on the correlation curve. Figure 19 shows that use of a filter optimized for the scale change in the sensed image can restore the correlation peak to values required for full confidence in a pattern match. The shape of the correlation curve in Figure 19 is significant because the secondary peak, present in Figure 18 when the filter was not optimized, is reduced. The secondary peak in Figure 18 represents a partial match caused by energy present in the window of the ln (R),θ image. The location of the secondary peak is at the center of the correlation plane, as expected, and represents a match between the reference and sensed windows. Figure 19 also shows that the level of Gaussian noise necessary to reduce the correlation peak below .7 is higher when the sensed filter is optimized for scale change.

Demonstration of Insensitivity to Window

The results shown in Figure 19 caused concern that most of the amplitude observed in the correlation peaks of Figures 16 through 19 was caused by the window, or frame size, of the sensed image. The scaling algorithm used to produce precisely scaled sensed imagery also served to scale precisely the image window by the same factor. Since the position of the secondary peak did not change with the

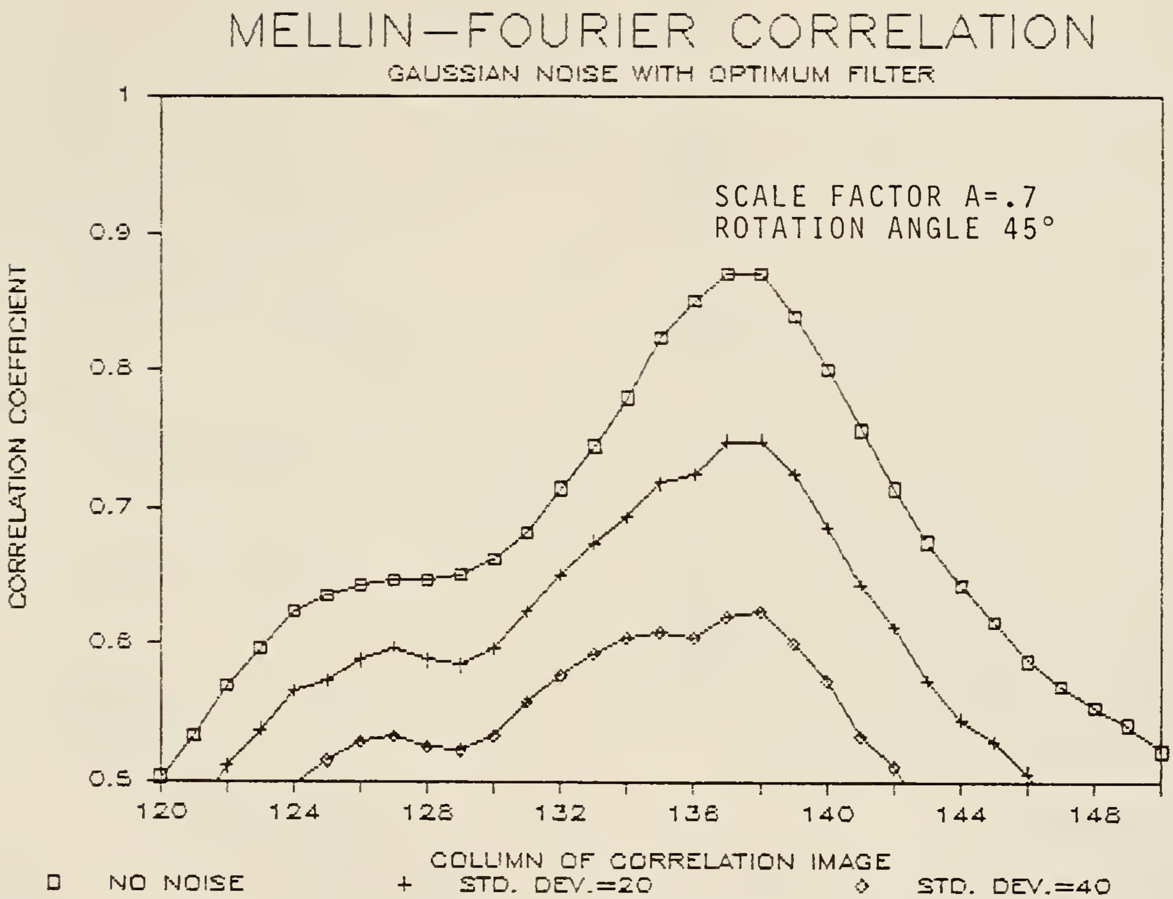

Figure 19. Gaussian distributed noise added to the sensed image. Added noise was zero mean, with the three standard deviations shown. Spatial filter optimized to the scale change in the sensed image.

scaling factor of the sensed image, it was considered likely that correlation amplitude was generated by the ln (R),θ window size, which was independent of the object scaling factor. An experiment was performed to demonstrate that the correlation peak was indicating the correct scale change and degree of similarity between the reference image and the sensed image. The Mellin-Fourier system was made to perform a correlation between the usual reference image and an incorrect sensed image. The incorrect sensed image was scaled by a factor of A = .7 and the filter bandpass was optimized for this scale change. The resulting correlation peak was not expected to indicate the proper scale factor nor was it expected to have sufficient amplitude to indicate a pattern match. The amplitude of the correlation peak was .662, well below the threshold for match, and the X position of the correlation peak indicated a scale factor of .85. These results indicate that the amplitude and position of the correlation peak are reliable indicators of pattern match and scale factor, and are not completely determined by image window size.

CHAPTER V
CONCLUSIONS

The numerical experiments described in this paper have shown how several issues can affect the evaluation of the space bandwidth requirements of a scale invariant correlation system. Spectral resolution and Nyquist sampling were seen to be the two main determinants of the space bandwidth required to achieve correlator invariance over a given range of scale change. Other things, such as windowing and truncation of the Fourier transform plane, were shown to have an effect on the validity of the cross correlation image.

Calculations done under the assumptions used by Anderson and Callary (4) were used to see how savings in system space bandwidth could be realized by careful choice of geometric transformation parameters. Further refinements of the choice of transformation parameters were applied in the development of the technique of range adaptive bandpass.

The series of examples presented in the section discussing optimum sampling for scale invariance showed how each of the principles described in the preceding sections

could be used successfully to restore the amplitude of the cross correlation peak in a scale invariant correlator.

The theoretical scaling limits of a Mellin-Fourier correlator were calculated and a computer simulation was used to verify that the theoretical benefits of range adaptive filtering could be applied in practice. Using only the techniques of range adaptive sampling and careful choice of transformation parameters, the scale invariance of the Mellin-Fourier correlator was extended by a factor of 5 for scaling factors less than 1.0 without increasing the space bandwidth of the system. The performance of the Mellin-Fourier correlator which used a range adaptive filter was similar to the fixed filter correlator when the scaling factor A was greater than 1.0.

Design approaches were suggested for systems required only to detect scale and rotation changes in a sensed image rather than to perform a detailed measure of pattern match. Range adaptive filtering techniques were seen to provide accurate measures of scale and rotation changes even though scale changes in the sensed image had violated Nyquist sampling conditions.

The techniques developed for Mellin-Fourier correlation were tested in an investigation of the benefits of higher space bandwidth. The effect of the larger format 256 X 256

frame was to increase the system space bandwidth by a factor of four. When standard scale invariant techniques were applied to the large format frame in the same way as with the 128 X 128 image, the larger space bandwidth produced a modest improvement in the correlation peak; not a significant improvement considering the large price paid in increasing the system space bandwidth. When range adaptive techniques were applied to the Mellin-Fourier correlator using the larger frame size, the correlation peak value still did not show a significant increase. These experiments suggest that signal processing techniques such as range adaptive transformations and spatial filtering contribute more to the success of the Mellin-Fourier correlator than an increase in correlator space bandwidth. The experiments further suggest that the theory for predicting performance of Mellin-Fourier correlator may be based on the well-established principles of Nyquist sampling and spectral resolution.

Investigations into the sensitivity of the Mellin-Fourier correlator to noise measured the influence of both uniform and Gaussian noise distributions on the value and position of the correlation peak. Higher space bandwidths were investigated and sensitivity to added noise was evaluated using the space bandwidth available in a 256 X 256 frame. Optimal choice of the spatial filter used

in processing the sensed image made the Mellin-Fourier correlator less sensitive to Gaussian noise. Experiments with incorrectly matched library images verified that the correlator was not simply responding to the scaled window through which the sensed image was viewed.

REFERENCES

1. Cassasent, D., & Psaltis, D. (1978). Deformation Invariant, Space Variant Optical Processing. In E. Wolf (Ed.), Progress in Optics, 16, (pp. 291-356). New York: North-Holland Publishing Company.

2. Cassasent, D., & Psaltis, D. (1976, July). Position, Rotation, and Scale Invariant Optical Correlation. Applied Optics, 15(7), 1795.

3. Cassasent, D., & Psaltis, D. (1977, June). Space Bandwidth Product and Accuracy of the Optical Mellin Transform. Applied Optics, 16(6), 1472.

4. Anderson, R.C., & Callary, P.R. (1981, April). Space Bandwidth Product for the Mellin Transform. Applied Optics, 20(8), 1272.

5. Horev, H. (1980,December). Picture Correlation Model for Automatic Machine Recognition, 7. Unpublished master's thesis, Air Force Institute of Technology, Wright-Patterson Air Force Base, OH.

6. Childers, D., & Durling, A. (1975). Digital Filtering and Signal Processing. (pp. 290-314). New York: West Publishing Company.

7. Childers, D., & Durling, A. (1975). Digital Filtering and Signal Processing. (p. 302). New York: West Publishing Company.

8. Anderson, R.C., & Callary, P.R. (1981, April). Space Bandwidth Product for the Mellin Transform. Applied Optics, 20(8), 1272.

9. Anderson, R.C., & Callary, P.R. (1981, April). Space Bandwidth Product for the Mellin Transform. Applied Optics, 20(8), 1272.

10. Cassasent, D., & Psaltis, D. (1977, June). Space Bandwidth Product and Accuracy of the Optical Mellin Transform. Applied Optics, 16(6), 1472.

BIOGRAPHICAL SKETCH

Mr. Friday graduated from the University of Alabama in 1973 with a Master of Science in Electrical Engineering. From 1974 to 1978 he served as a system engineer for an airborne infrared measurement system operated by the U. S. Air Force at Eglin Air Force Base, Florida. He was selected by the Air Force to attend the University of Florida for long-term, full-time study where he was admitted to candidacy for the PhD degree. In 1978 he joined the Air Force Armament Laboratory where he was program manager for projects involving computer generation of synthetic infrared images. From 1981 to 1983, he received funding from the Air Force Office of Scientific Research (AFOSR) to do basic research in pattern recognition using Mellin transforms. He is now employed by E G & G Special Projects Inc., in Las Vegas, Nevada, and is continuing studies of computer simulations of electro-optical pattern recognition algorithms.

I certify that I have read this study and that in my opinion it conforms to acceptable standards of scholarly presentation and is fully adequate, in scope and quality, as a dissertation for the degree of Doctor of Philosophy.

Roland C. Anderson
Professor, Department of Engineering Sciences

I certify that I have read this study and that in my opinion it conforms to acceptable standards of scholarly presentation and is fully adequate, in scope and quality, as a dissertation for the degree of Doctor of Philosophy.

Ulrich H. Kurzweg
Professor, Department of Engineering Sciences

I certify that I have read this study and that in my opinion it conforms to acceptable standards of scholarly presentation and is fully adequate, in scope and quality, as a dissertation for the degree of Doctor of Philosophy.

Alex E. Green
Graduate Reasearch Professor, Department of Physics

I certify that I have read this study and that in my opinion it conforms to acceptable standards of scholarly presentation and is fully adequate, in scope and quality, as a dissertation for the degree of Doctor of Philosophy.

Stanley S. Ballard
Distinguished Service Professor, Department of Physics

I certify that I have read this study and that in my opinion it conforms to acceptable standards of scholarly presentation and is fully adequate, in scope and quality, as a dissertation for the degree of Doctor of Philosophy.

Knox Millsaps
Professor and Chairman, Department of Engineering Sciences

I certify that I have read this study and that in my opinion it conforms to acceptable standards of scholarly presentation and is fully adequate, in scope and quality, as a dissertation for the degree of Doctor of Philosophy.

Richard L. Fearn

Richard L. Fearn
Professor, Department of Engineering Sciences

This dissertation was submitted to the Graduate Faculty of the College of Engineering and to the Graduate School and was accepted as partial fulfillment of the requirements for the degree of Doctor of Philosophy.

May 1985

Herbert A. Bevis

Herbert Bevis
Dean, College of Engineering

Madelyn Lockhart
Dean, Graduate School